

CHARACTERIZATION OF HEAT SINK FLOW BYPASS IN PLATE FIN HEAT SINKS

W. Leonard, P. Teertstra, J.R. Culham
Microelectronics Heat Transfer Laboratory
Department of Mechanical Engineering
University of Waterloo
Waterloo, Ontario
Canada N2L 3G1
Email: willy@mhtlab.uwaterloo.ca

Ahmed Zaghol
R-Theta Inc.
Mississauga, Ontario
Canada, L5T 1Y9

ABSTRACT

Experimental testing has been performed on two plate fin heat sinks in order to examine flow bypass phenomenon. The present study examines pressure drop and thermal resistance as well as flow velocities within the heat sinks. Tests are performed for bypass channel/fin height ratios of 0.25, 0.5, 0.75 and 1 with approach velocities from 2 to 8 m/s.

By examining flow behavior within the heat sinks and the bypass channel, a model for predicting flow bypass is presented that incorporates only the significant pressure drop mechanisms that affect the flow path. This model allows for a simple prediction of flow bypass for plate fin heat sinks based solely on geometry. For all of the heat sinks tested the agreement between model and experimental data is \mp 8%.

L heat sink length, m
Q energy transfer or flow rate, W or m^3/s
R thermal resistance, $^{\circ}C/W$
Re_c heat sink channel Reynolds number
Re_d duct Reynolds Number
s fin separation, m
t fin thickness, m
T_{avg} average baseplate temperature, $^{\circ}C$
T_{amb} ambient temperature, $^{\circ}C$
U_a approach velocity, m/s
U_h heat sink average velocity, m/s
U_{lk} heat sink average leakage velocity, m/s
U_s stagnation velocity, m/s
ΔP pressure drop, Pa

NOMENCLATURE

A_d duct area, m^2
A_{hs} heat sink frontal area, m^2
A_{lk} heat sink leakage area, m^2
b heat sink base plate thickness, m
C_b bypass channel width, m
d_{h,h} heat sink channel hydraulic diameter, m
d_{h,d} duct hydraulic diameter, m
f friction factor
H fin height, m
l effective frictional flow length, m

Greek Symbols

ρ mass density, kg/m^3
 ν kinematic viscosity m^2/s

Subscripts

a approach
h heat sink
lk leakage
d duct
b bypass

INTRODUCTION

As power dissipation levels increase in electronics applications the role of heat transfer enhancements, such as heat sinks, serve a much more important role in thermal management strategies. While many models are available for predicting thermal behavior in plate fin heat sinks, most are constrained to shrouded conditions at the external boundaries to eliminate flow bypass. Although this assumption simplifies the analysis procedure it is not representative of most heat sink configurations found in electronics applications. Analyses employing this assumption tend to over estimate thermal performance resulting in an undersized heat sink. Most existing models for flow bypass do not accurately predict flow conditions, but rather focus on determining the pressure drop associated with the problem in order to back out the thermal resistance from the zero bypass pressure drop curve. Other models depend on knowing the bypass associated with the problem in order to determine the flow conditions.

The effects of flow bypass on heat sink thermal performance have been investigated experimentally, numerically and analytically in the literature.

Experimentally, Sparrow and co-workers [1-3] investigated the effects of tip bypass on the pressure drop characteristics and thermal performance of plate fin and pin fin heat sinks. Lau and Mahajan [4] examined tip bypass in rectangular and convoluted fins. Lee et al. [5] considered thermal performance in plate fin heat sinks with both tip and lateral clearance. Azar and Mandrone [6] studied the effects of pin fin density on thermal resistance under flow bypass. Shaukatullah and Gaynes [7] examined the thermal resistance of pin fin heat sinks in open flow. Wirtz et al. [8] investigated plate fin heat sinks with tip bypass and developed a correlation which relates the heat sink flow rate to the approach rate and heat sink fin density. Chapman et al. [9] considered plate fin, strip fin and elliptical pin fin heat sinks in open flow. More recently, Jonsson and co-workers [10-12] studied plate fin, pin fin and strip fin heat sinks and developed an empirical bypass correlation. In general, most experimental studies involved measuring only the pressure drop and thermal resistance associated with a particular problem. This study will examine the actual flow patterns generated within the heat sink and the bypass channel in order to accurately characterize the flow domain.

Analytically, Lee [13] and Simons and Schmidt [14] developed models based on momentum and mass balance to predict bypass performance. Butterbaugh and Kang [15] and Jonsson and Palm [12] developed pressure balance models to predict thermal performance based on pressure drop.

Barret and Obinelo [16] examined the ability of numerical methods to predict bypass performance. Sata et al. [17], Obinelo [18], Radmehr et al. [19] and Prstic et al. [20] investigated plate fin thermal performance under bypass conditions numerically.

In this paper, the results of an experimental and analytical investigation of the thermal performance of two heat sinks in the presence of tip bypass are investigated. Tip bypass was examined

for the bypass channel width to fin height ratios (C_b/H) from 0.25 to 1 for free stream approach velocities from 2 to 8 m/s. Velocity measurements were made across the heat sink channels and into the bypass channel at various points along the heat sink in order to compare the actual heat sink flow rates to those estimated from thermal resistance comparisons at zero bypass. It was determined that estimating average flow through the heat sink by using zero bypass thermal resistance data is satisfactory. Also, a physical bypass model based on that developed by Butterbaugh and Kang [14] and modified to reflect the observations seen in the measured flow patterns is put forth and compared to experimental data.

EXPERIMENTAL PROCEDURE

Test Samples

Two heat sinks were examined in this study. The heat sinks produced by R-Theta of Mississauga, Ontario were constructed by swaging copper sheets into a copper baseplate, both with a thermal conductivity of approximately 300 W/mK. A schematic diagram of a general, plate fin heat sink, representative of the heat sinks used in this study, is shown in Fig. 1.

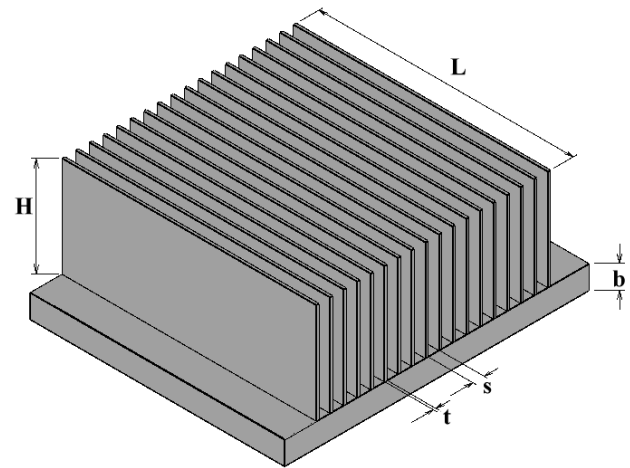


Figure 1. GENERAL HEAT SINK

The relevant dimensions for each of the heat sink samples in this study are shown in Table 1.

All references to heat sinks 1 and 2 will correspond to samples 1 and 2, respectively as given in Table 1.

Test Apparatus

In order to minimize heat losses and accurately measure heat dissipation from the heat sink, matching pairs of each heat sink were configured in a back-to-back configuration as shown in Fig. 2. The heat sinks were firmly bolted to heater plates using

Table 1. TEST SAMPLE DIMENSIONS (mm)

Sample	H	L	s	t	b
1	49.8	127	2.1	1.2	12.7
2	50.3	127	4.2	1.2	12.7

four countersunk machine screws at an equal distance from the center of the heater plate, as represented by the schematic in Fig. 3.

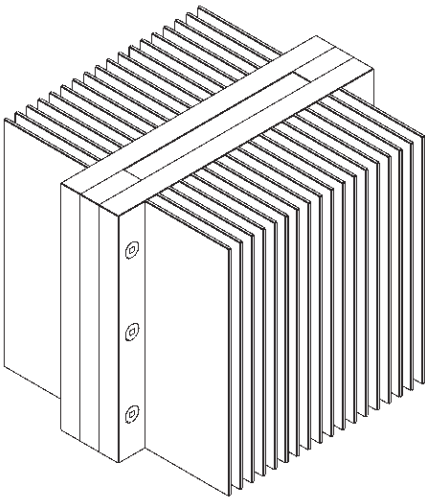


Figure 2. HEAT SINK BACK TO BACK CONFIGURATION

Each of the bolts were torqued to $2.25 \text{ N} \cdot \text{m}$ (20 in · lbs) using a consistent bolting pattern for all of the tests. The heat sinks were bolted together using six countersunk machine screws at equal intervals on the extruding edges of the assembly. A three sided phenolic spacer was bolted between the heat sinks to minimize convection from the heater plates, as shown in Fig. 2. Four 200 W cartridge heaters were press fitted into four wells drilled into the heater plates, shown in Fig. 4.

Thermal grease was used in the interface between the heat sinks and the heater plates. Because of the symmetry of the assembly, it was assumed that the heat dissipated by the cartridge heaters was equally distributed between the two heat sinks. The heaters were powered using a Xantrex 150-7 DC power supply and typical line voltages of 120V at a current of approximately 6.6 A were supplied to the heaters.

Temperature measurements were performed using 5 mil T-type copper-constantan thermocouples with Teflon coating connected to a Keithley 2700 data acquisition system. Because of the small diameter of the thermocouple wires and the relatively large

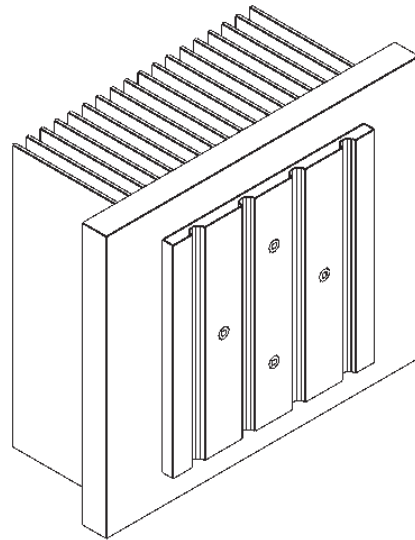


Figure 3. HEAT SINK AND HEATER PLATE

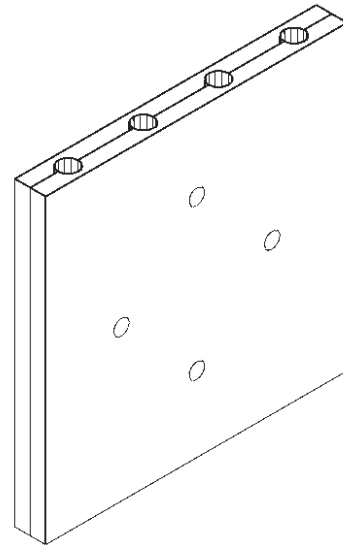


Figure 4. HEAT SINK AND HEATER PLATE

values of overall power dissipation, conductive losses through the leads were assumed to be negligible. Ambient temperatures in the test section were monitored using two thermocouples mounted just outside the main flow corridor.

It was assumed that the spreading resistance between the heater plate and base plate was negligible and the heater plate temperature was taken as the base plate temperature. The heater plate temperature was measured in four interior locations on each of the heater plates indicated by locations T1-T4 in Fig. 5. The thermocouples were located on the heater plate so that an arithmetic average of their measured values would provide a repre-

sentative value for the mean plate temperature.

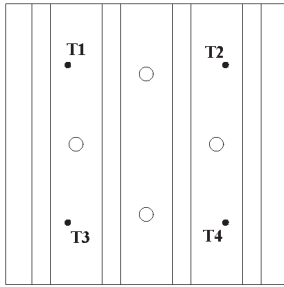


Figure 5. HEATER PLATE THERMOCOUPLE LOCATIONS

In order to vary the tip bypass, the heat sink assembly was placed inside a specially designed Plexiglas shroud, as shown in Fig. 6. The two walls facing the fin tips were easily movable to allow a bypass channel from 0 to 50 mm. The side dimensions of the shroud were set to approximately one channel width larger than the heat sink on all sides. The shroud and heat sink assembly were suspended at the center of a 450 mm x 450 mm vertical wind tunnel and the space between the outside of the shroud and the wind tunnel walls was blocked to control airflow through the assembly. The approach velocity to the heat sink assemblies was measured using a Dantec hot wire anemometer placed approximately 80 mm upstream of the leading edge of the heat sink assembly.

The pressure drop across the heat sinks was measured approximately 25 mm upstream from the leading edge to 25 mm downstream from the trailing edge using two Dwyer differential pressure transducers. The first transducer measured pressure drops between 0 and 250 Pa and the second measured pressure drops between 0 and 1250 Pa. The second transducer was only used when the pressure drop exceeded 250 Pa.

In order to measure inter-fin velocities throughout the length and width of the heat sink, a small slit was cut into the shroud and a 400 mm linear translation station was mounted on the outside, as shown in Fig. 6. 90° angled pitot probes of five different lengths were mounted on the translation station and were used to determine velocity profiles at the inlet, exit, at 25 mm from both the inlet and exit and at the midpoint of the heat sink.

The overall uncertainty of experimental results was estimated using a procedure outlined by Moffat[21] and Helmes [22] and the influence on reported results is shown in Table 2.

Test Procedure

Experimental testing was performed for free stream approach velocities of 2, 3, 4, 5, 6, 7 and 8 m/s for bypass channel to fin height ratios of 0, 0.25, 0.5, 0.75 and 1 of fin height. At 2, 4 and 6 m/s approach velocities at bypass ratios of 0.5 and 1, pitot

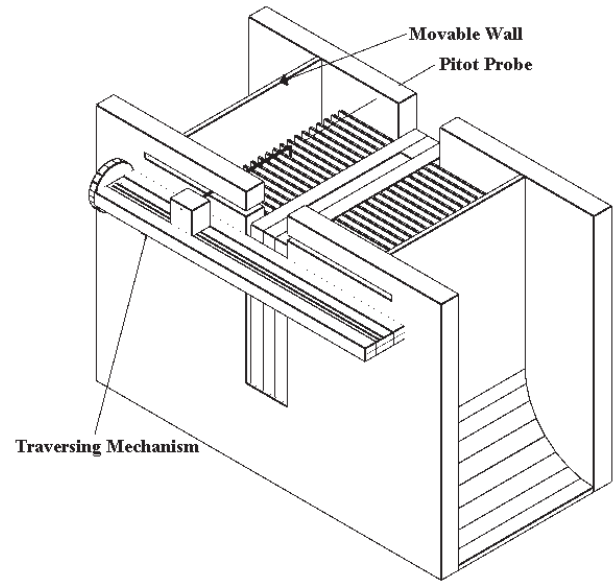


Figure 6. HEATER PLATE THERMOCOUPLE LOCATIONS

Table 2. Experimental Uncertainty

Reported Result	Max Error (%)	RMS Error (%)
R (°C/W)	1.35	0.94
Re	3.32	2.96
U_s	3.58	2.95
Interfin Velocities	24.85	12.02

probe traverses of the fin channel and into the bypass channel were made at 0, 20, 50, 80 and 100% of the heat sink's length.

Air was the working fluid in the testing and a steady state, steady flow condition was assumed while measurements were taken. Steady state was assumed once all of the thermocouples had reached a convergence of less than a 0.1°C change in temperature over 20 time steps (200 seconds) and no observable temperature trend existed.

RESULTS AND DISCUSSION

Expressions

In the following sections, a non dimensional Reynolds duct number is used in order to present the data in a normalized form, this Reynolds number is expressed as:

$$Re_d = \frac{d_d \cdot U_a}{\nu} \quad (1)$$

where,

$$d_d = \frac{4 \cdot \text{duct area}}{\text{duct perimeter}} \quad (2)$$

Inter-fin Velocities

Inter-fin velocities are in general only known at the zero bypass condition. By assuming that for equal thermal resistance for a particular heat sink under different bypass conditions that an equal average inter-fin velocity exists, we are able to estimate the average inter-fin velocity for each test case. These results were compared to the average inter-fin velocities determined by the pitot probe flow traverses. This comparison can be seen in Figs. 7 and 8 for heat sinks 1 and 2, respectively.

From these figures, we can see that the pitot probe traverse and thermal resistance determination of the inter-fin velocities are in good agreement, with the largest difference being 8% with the average difference around 3%. This indicates that backing out the average inter fin velocity from the zero bypass resistance curve is an adequate assumption for the average flow through the heat sink under bypass conditions.

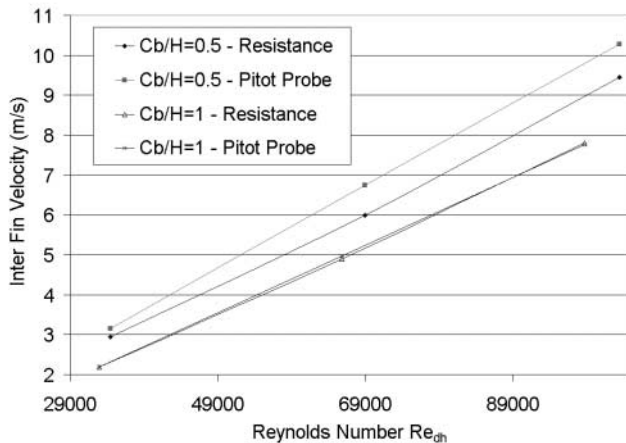


Figure 7. INTER FIN VELOCITY COMPARISON - SAMPLE 1

BYPASS MODEL

The following model is a modified version of the pressure balance model presented by Butterbaugh and Kang [15].

Butterbaugh and Kang presented a model in which all pressure drop contributions along the bypass channel are equated to all of the pressure drops along the heat sink path. More specifically, the sum of the stagnation pressure rise and the heat sink

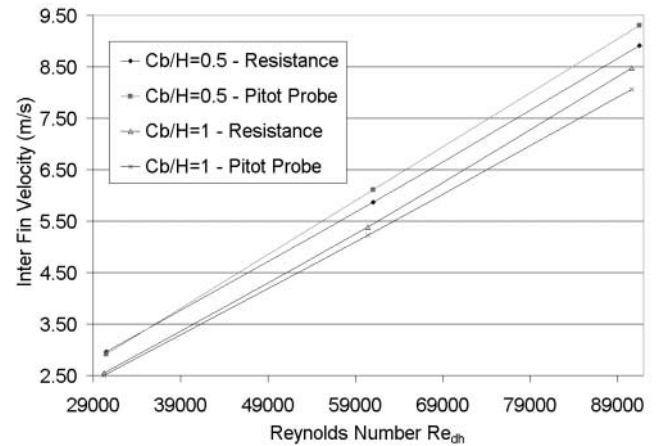


Figure 8. INTER FIN VELOCITY COMPARISON - SAMPLE 2

inlet, frictional and exit pressure drops were balanced with the inlet, frictional and exit pressure drops along the bypass channel and the frictional pressure drop associated with flow from the heat sink into the bypass channel. The idea of this model was to predict the pressure drop across the heat sink in order to determine the thermal resistance from the zero bypass case.

In the current model, we recognize that the largest contributor to flow entering the bypass channel is the pressure drop associated with flow through the heat sink. Inlet and exit effects are neglected and a pressure drop balance between the flow passing through the heat sink and the flow leaking through the top of the heat sink into the bypass channel is used to determine the average flow through the heat sink.

At the heat sink inlet, the flow is subject to three pressure changes, the stagnation pressure rise associated with the reduction in area, and the pressure drops associated with the heat sink and bypass channel entrances. In general, the pressure change due to stagnation is much higher than either of the entrance effects. For this reason, we will assume that the entrance velocity into both the heat sink and bypass channel is the stagnation velocity.

$$U_s = \frac{U_a \cdot A_d}{A_d - A_{hs}} \quad (3)$$

The measured values of the entrance velocities from the pitot probe traverses support this assumption.

Air entering the leading face of the heat sink can follow one of two paths, through the channels formed by the plate fins or through the top surface of these channels and into the bypass region. By equating the pressure drops associated with each path we are able to determine the amount of flow that continues to the trailing edge of the heat sink and the amount of flow that leaks

into the bypass channel.

Given the governing equations for the mass balance and pressure balance:

$$Q_a = Q_h + Q_{lk} \quad (4)$$

$$\Delta P_h = \Delta P_b + \Delta P_{lk} \quad (5)$$

Solving Eqs. 4 and 5 gives the average heat sink velocity U_h and the average leakage velocity U_{lk} , where the frictional pressure drops are given by:

$$\Delta P = \frac{1}{2} \frac{f \cdot l \cdot \rho \cdot U^2}{d_h} \quad (6)$$

and the friction factors are given by:

$$f = \begin{cases} \frac{24}{Re} & \text{if } Re < 2300 \\ \left[\left(\frac{0.1268}{Re^{0.3}} \right)^4 - \left(\frac{24}{Re} \right)^4 \right]^{1/4} & \text{if } 2300 < Re < 5000 \\ \frac{0.1268}{Re^{0.3}} & \text{if } Re > 5000 \end{cases}$$

The Reynolds number, Re is calculated as:

$$Re = \frac{d_h \cdot U}{\nu} \quad (7)$$

where the hydraulic diameter for the bypass channel was given by equation [1] and the hydraulic diameter through the heat sink is:

$$d_{h,h} = 2 \cdot s \quad (8)$$

In solving the pressure balance, we need to determine l and U for the heat sink, and both portions of the bypass flow paths.

For the flow through the heat sink, we make $l = L$ and $U = U_{hs}$.

Using geometry, we can express the average path length of the bypass flow through the heat sink as:

$$l_{b,h} = \sqrt{\left(\frac{L}{\sqrt{2}} \cdot \frac{U_{lk}}{\frac{U_s - U_h}{2\sqrt{2}} + U_s} \right)^2 + \left(\frac{L}{\sqrt{2}} \right)^2} \quad (9)$$

and determine a corresponding velocity of:

$$U_{b,h} = \sqrt{\left(\frac{U_{lk}}{\frac{U_s - U_h}{2\sqrt{2}} + U_s} \right)^2 + U_{lk}^2} \quad (10)$$

and for the flow into the bypass channel, we have:

$$l_b = L - \frac{L}{\sqrt{2}} \quad (11)$$

and,

$$U_{b,b} = (2 + \sqrt{2}) \cdot U_b - (1 + \sqrt{2}) \cdot U_s \quad (12)$$

In solving the mass balance equation we set:

$$Q_a = \text{duct height} \cdot \text{duct width} \cdot U_a \quad (13)$$

$$Q_h = U_h \cdot s \cdot N \cdot H \quad (14)$$

and

$$Q_{lk} = U_{lk} \cdot A_{lk} \quad (15)$$

where,

$$A_{lk} = s \cdot (N - 1) \cdot L \quad (16)$$

At the heat sink exit, there are pressure drops associated with the heat sink and bypass channel exits as well as the pressure drop associated with the increase in flow area. All of these pressure drops are quite small in comparison to the frictional pressure drop through the heat sink and as a result have a negligible effect on the flow paths.

Evaluation of Bypass Model

The bypass model previously described has been compared to the experimental data as well as to the physical bypass model described by Jonsson and Palm [12]. This comparison can be seen in Figs. 9 to 12. Results are given for bypass channel to fin height ratios of 0.25 and 0.75.

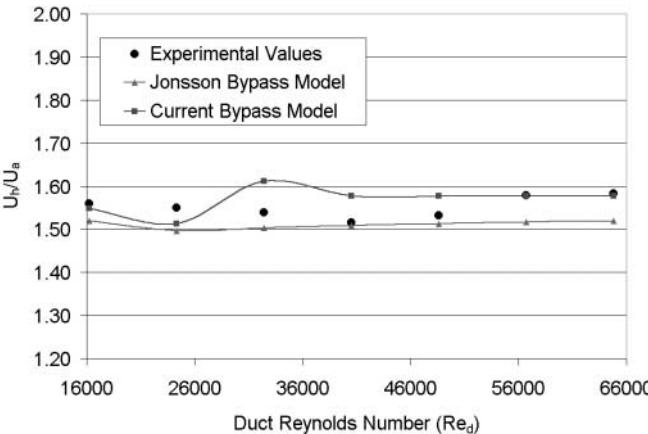


Figure 11. MODEL EVALUATION - SAMPLE 2 - $\frac{C_b}{H} = 0.25$

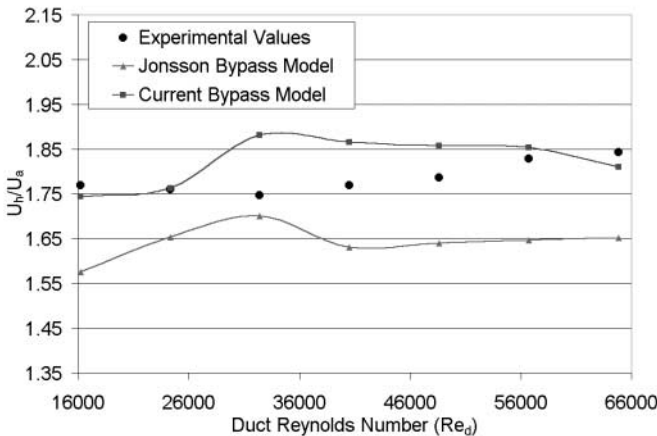


Figure 9. MODEL EVALUATION - SAMPLE 1 - $\frac{C_b}{H} = 0.25$

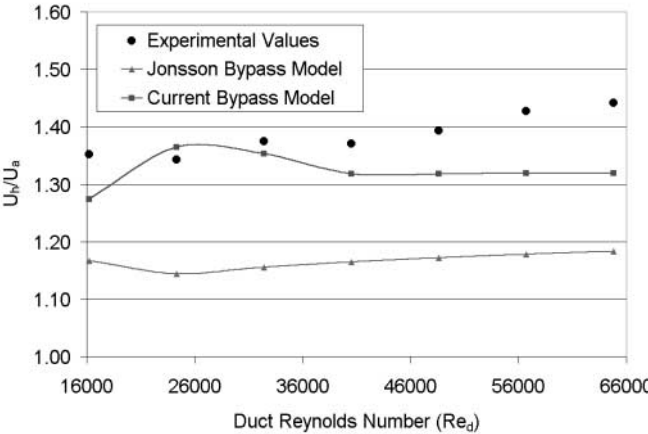


Figure 12. MODEL EVALUATION - SAMPLE 2 - $\frac{C_b}{H} = 0.75$

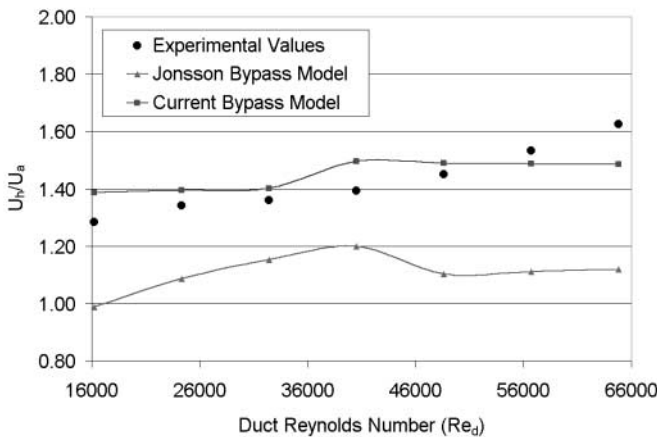


Figure 10. MODEL EVALUATION - SAMPLE 1 - $\frac{C_b}{H} = 0.75$

From these results, we can see that for both heat sinks, the model accurately predicts the experimentally obtained data with a maximum and RMS error of 8% and 5%. For Jonsson’s model, we can see varying degrees of agreement with the experimental data. Generally, Jonsson’s model predicts within 25% of the experimentally obtained data.

CONCLUSIONS

In this report an experimental study was performed to examine flow bypass. A simple bypass model based solely on heat sink geometry is proposed in order to predict average flow velocities through a heat sink subject to flow bypass. The model

is able to predict flow distribution under the test cases examined within 8% accuracy.

ACKNOWLEDGMENTS

The authors gratefully acknowledge Materials and Manufacturing Ontario and the Natural Science and Engineering Research Council of Canada for their continued support of this work.

REFERENCES

1. Sparrow, E. M., Baliga, B. R., Patankar, S.V., "Forced Convection Heat Transfer from a Shrouded Fin Array with and without Tip Clearance", *ASME J. Heat Transfer*, Vol. 100, Nov. 1978, pp. 572-579.
2. Sparrow, E. M., Beckey, T. J., "Pressure Drop Characteristics for a Shrouded Longitudinal-Fin Array with Tip Clearance", *ASME J. Heat Transfer*, Vol. 103, May 1981, pp. 393-395.
3. Sparrow, E. M., Kadle, D. S., "Effect of Tip-to-Shroud Clearance on Turbulent Heat Transfer from a Shrouded, Longitudinal Fin Array", *ASME J. Heat Transfer*, Vol. 108, August 1986, pp. 519-524.
4. Lau, K. S., Mahajan, R. L., "Effects of Tip Clearance and Fin Density on the Performance of Heat Sinks for VLSI Packages", *IEEE Trans. Components, Hybrids, and Manufacturing Technology*, Vol. 12, No. 4, December 1989, pp. 756-765.
5. Lee, R. S., Huang, H. C., Chen, W. Y., "A Thermal Study of Extruded Type Heat Sinks in Considering Air Flow Bypass Phenomenon", *Proc. Sixth IEEE Semi-Therm Symposium*, 1990, pp. 95-102.
6. Azar, K., Mandrone, C. D., "Effect of Pin Fin Density of the Thermal Performance of Unshrouded Pin Fin Heat Sinks", *ASME J. Electronic Packaging*, Vol. 116, December 1994, pp. 306-309.
7. Shaikatullah, H., Gaynes, M. A., "Effect of Pin Fin Heat Sink Size on Thermal Performance of Surface Mount Plastic Quad Flat Packs", *Proc. 1994 Int. Electronics Packaging Conference*, Atlanta, September 1994, pp. 232-241.
8. Wirtz, R. A., Chen, W., Zhou, R., "Effect of Flow Bypass on the Performance of Longitudinal Fin Heat Sinks", *ASME J. Electronic Packaging*, Vol. 116, September 1994, pp. 206-211.
9. Chapman, C. L., Lee, S., Schmidt, B. L., "Thermal Performance of an Elliptical Pin Fin Heat Sink", *Proc. Tenth IEEE Semi-Therm Symposium*, San Jose, February 1994, pp. 24-31.
10. Jonsson, H., Palm B., "Influence of of Airflow Bypass on the Thermal Performance and Pressure Drop of Plate Fin and Pin Fin Heat Sinks for Electronics Cooling", *Proc. Eurotherm Sem. No. 58*, Nantes, France, September 1997, pp. 44-50.
11. Jonsson, H., Palm B., "Thermal and Hydraulic Behavior of Plate Fin and Strip Fin Heat Sinks Under Varying Bypass Conditions", *Proc. 1998 Intersociety Conf. On Thermal and Thermomechanical Phenomena in Electronic Systems (ITherm '98)*, Seattle, May 1998, pp. 96-103.
12. Jonsson, H., Moshfehg, B., "Modeling of the Thermal and Hydraulic Performance of Plate Fin, Strip Fin, and Pin Fin Heat Sinks - Influence of Flow Bypass", *Proc. 2000 Intersociety Conf. on Thermal Phenomena (ITherm 2000)*, Las Vegas, May 2000, pp. 185-192.
13. Lee, S., 1995, "Optimum Design and Selection of Heat Sinks", *IEEE Trans. Components, Packaging, and Manufacturing Technology - Part A*, Vol. 18, No. 4, December 1995, pp. 812-817.
14. Simons, R., Schmidt, R., "A simple Method to Estimate Heat Sink Air Flow Bypass", *Electronics Cooling*, Vol. 3, No. 2, May 1997 pp. 36-37.
15. Butterbaugh, M. A., Kang, S. S., "Effect of Airflow Bypass on the Performance of Heat Sinks in Electronic Cooling", *EEP-Vol. 10-2, Advances in Electronic Packaging*, 1995, pp. 843-848.
16. Barrett A. V., Obinelo, I. F., "Characterization of Longitudinal Fin Heat Sink Thermal Performance and Flow Bypass Effects Through CFD Methods", *Proc. Thirteenth IEEE Semi-Therm Symposium*, Austin, January 1997, pp. 158-164.
17. Sata, Y., Iwasaki, H., Ishizuka, M., "Development of Prediction Technique for Cooling Performance of Finned Heat Sink in Uniform Flow", *Proc. 1996 Intersociety Conference on Thermal Phenomena (ITherm 1996)*, Orlando, May-June 1996, pp. 108-114.
18. Obinelo, I. F., "Characterization of Thermal Performance of Longitudinal Fin Heat Sinks for System Level Modeling Using CFD Methods", *ASME Interpak'97 - Advances in Electronic Packaging*, Hawaii, June 1997.
19. Radmehr, A., Kelkar, K. M., Kelly, P., Patankar, S. V., "Analysis of the Effect of Bypass on the Performance of Heat Sinks Using Flow Network Modeling (FNM)", *Proc. Fifteenth IEEE Semi-Therm Symposium*, San Diego, March 1999, pp. 42-47.
20. Prstic, S., Iyengar, M., Bar-Cohen, A., "Bypass Effect in High Performance Heat Sinks", *International Thermal Sciences Conference*, Bled, Slovenia, June 2000.
21. R. J. Moffat, "Describing the Uncertainties in Experimental Results", *Experimental Thermal and Fluid Science*, No. 1, pp. 3-17, 1988.
22. J. Geremia, Eds. R. A. Granger, *Experiments in Fluid Mechanics*, Holt, Rinehart and Winston Inc, Appendix C, 1988.